Inorg. Chem. **2009**, *48*, 1844−1856

pH-Specific Synthetic Chemistry and Solution Studies in the Binary System of Iron(III) with the α-Hydroxycarboxylate Substrate Quinic Acid: Potential Relevance to Iron Chemistry in Plant Fluids

M. Menelaou,[†] C. Mateescu,[‡] H. Zhao,[§] I. Rodriguez-Escudero,[§] N. Lalioti,[||] Y. Sanakis,[⊥] A. Simopoulos,[⊥] and A. Salifoglou*[,†]

Department of Chemical Engineering, Aristotle University of Thessaloniki, Thessaloniki 54124, Greece, Department of Materials Science, University of Patras, Patras 26500, Greece, Department of Chemistry, University of Puerto Rico, San Juan, Puerto Rico 00931-3346, Institute of Materials Science, NCSR "Demokritos", Aghia Paraskevi 15310, Attiki, Greece, and Banat University of Agricultural Sciences and Veterinary Medicine, Timisoara 1900, Romania

Received February 25, 2008

Iron is an essential metal ion in plant growth and development. Mobilization and further use of that metal by cellular structures in metabolic pathways entails the existence of soluble forms complexed with indigenous organic substrates, such as the low molecular mass D-(-)-quinic acid. In an effort to understand the relevant aqueous chemistry involving well-defined forms of iron, research efforts were carried out on the binary Fe(III)-quinic acid system. pH-specific reactions of $FeCl_3 \cdot 6H_2O$ with quinic acid in a molar ratio 1:3 led to the isolation of the mononuclear Fe(III)-quinate complexes, $K[Fe(C_7H_{11}O_6)_3] \cdot (OH) \cdot 3H_2O$ (**1**), $(NH_4)[Fe(C_7H_{11}O_6)_3] \cdot (OH)$ (**2**), and $Na[Fe(C_7H_{11}O_6)_3] \cdot (OH) \cdot 8H_2O$ (**3**). Compounds **1**−**3** were characterized by analytical, spectroscopic techniques (UV/vis, FT-IR, Electron Paramagnetic Resonance (EPR), and Mössbauer spectroscopy), cyclic voltammetry, and magnetic susceptibility measurements. Compound **1** crystallizes in $P2_13$, with $a = 15.1693(9)$ Å, $V = 3490.6(4)$ Å^3, and $Z = 4$. Compound **2** crystallizes in $P2_13$, with $a = 15.2831(9)$ Å, $V = 3569.7(4)$ Å^3, and $Z = 4$. Compound **3** crystallizes in $P2_13$, with $a = 15.6019(14)$ Å, $V = 3797.8(6)$ Å^3, and $Z = 4$. The X-ray crystal structures of **1**−**3** reveal a mononuclear Fe(III) ion bound by three quinates in an octahedral fashion. Each quinate ligand binds Fe(III) through the α-hydroxycarboxylate group as a singly deprotonated moiety, retaining the alcoholic hydrogen. EPR measurements in solution suggest that **1** dissociates, releasing free quinate. Solution speciation studies of the binary system (a) unravel the aqueous species distribution as a function of pH and reagent molar ratio, and (b) corroborate the EPR results proposing the existence of a neutral Fe(III)-quinate complex form. The collective physicochemical properties of **1**−**3** formulate a well-defined profile for the Fe(III) assembly in aqueous media and project structural features consistent with solubilized Fe(III)-hydroxycarboxylate binary forms potentially mobilized into plant (bio)chemical processes.

Introduction

As an important transition metal, iron is found in many biological systems in all living organisms (bacteria, plants, and mammals).[1−3] As a nutritional metal, iron exists in all soils and consequently in plants. It is extremely important for their growth and development. In plants, iron is transported through the roots to the rest of the plant. Albeit the most abundant transition metal, its bioavailability under aqueous−aerobic conditions and specific pH-conditions is limited because of the formation of insoluble iron oxides and iron hydroxides. Therefore, for iron to actively participate in biochemical processes,[4] it must exist in soluble and bioavailable forms across the physiological pH range. These forms arise through interactions of iron with chelates (organic

* To whom correspondence should be addressed. E-mail: salif@auth.gr. Phone: +30-2310-996-179. Fax: +30-2310-996-196.
[†] Aristotle University of Thessaloniki.
[‡] Banat University of Agricultural Sciences and Veterinary Medicine.
[§] University of Puerto Rico.
[||] University of Patras.
[⊥] NCSR "Demokritos".

10.1021/ic800356v CCC: $40.75
Published on Web 01/27/2009

substrates) in the cytosol or in the extracellular fluids. To this end, organic acid metal chelators have been found to be generated in plants and to contribute to iron solubility and bioavailability.

An efficient low molecular mass organic acid chelator in plants is D-(-)-quinic acid, 1α,3α,4α,5β-tetrahydroxy-1-cyclohexane carboxylic acid. There, it is encountered as a precursor to shikimic acid[5] involved in the biosynthesis of many natural products, which contain an aromatic ring, including essential amino acids and folic acid.[6] Therefore, the presence of quinic acid appears to be vital to plant cellular physiology,[7] with the organic acid capable of binding metal ions in relevant fluids. Quinic acid contains two very important features: (a) a carboxylate moiety, known to promote metal ion binding, (b) one alcoholic group in a position α- to the carboxylate group, and (c) three additional alcoholic groups relevant to polyol functionalities. These structural attributes are essential in promoting metal ion binding chemistry in plant fluids. In this sense, coordination of quinic acid to a metalloelement, such as Fe(III), promotes solubilization and contributes to the (bio)availability of Fe(III), leading to metallo(bio)chemical interactions essential to cellular function.

Being cognizant of the importance of such metallo(bio)-chemical activity in plant fluids and the absence of well-defined and characterized binary Fe(III)-quinic acid species present in such fluids, we launched research efforts targeting requisite synthetic and solution studies. To this end, the exploration of the binary system of Fe(III)-quinic acid aims at unravelling key aspects of the corresponding aqueous structural speciation relevant to cellular physiology in plants. Herein, we report on the pH-specific synthesis and isolation of the first soluble binary Fe(III)-quinate complexes with distinct spectroscopic, magnetic susceptibility, solid state, and aqueous solution properties.

Experimental Section

Materials and Methods. All experiments were carried out in aqueous media under aerobic conditions. Nanopure quality water was used for all reactions. $FeCl_3 \cdot 6H_2O$, $Fe(NO_3)_3 \cdot 9H_2O$, and D-(-)-quinic acid were purchased from Fluka. Ammonia, NaOH and KOH were supplied by Aldrich.

Physical Measurements. Fourier transform-infrared spectra (FT-IR) were recorded on a Perkin-Elmer 1760X FT-infrared spectrometer. UV/vis measurements were carried out on a Hitachi U2001 spectrophotometer in the range from 190 to 1000 nm. A ThermoFinnigan Flash EA 1112 CHNS elemental analyzer was used for the simultaneous determination of carbon, hydrogen, and nitrogen (%). The analyzer is based on the dynamic flash combustion of the sample (at 1800 °C) followed by reduction, trapping, complete GC separation, and detection of the products. The instrument was fully automated and controlled by PC via the Eager 300 dedicated software. A major advantage of the instrument is that it can handle solid, liquid, or gaseous substances. Further quantitative analyses for chloride content in the derived compounds were carried out by (a) Galbraith Laboratories, Inc., and (b) wet quantitative titrimetric determination, according to known procedures (Mohr's method).

The Electron Paramagnetic Resonance (EPR) spectra of complex **1** in the solid state and in aqueous solutions were recorded on a Bruker ER 200D-SRC X-band spectrometer, equipped with an Oxford ESR 9 cryostat at 9.61 GHz, 10 dB (2 mW) and at 4 K. Magnetic susceptibility data were collected on powdered samples of **1** with a Quantum Design SQUID susceptometer in the 2−300 K temperature range, under various applied magnetic fields. Magnetization measurements were carried out at three different temperatures in the field range 0−5 T.

Zero-Field Mössbauer spectra from polycrystalline samples of **1** were recorded with the conventional constant acceleration method, using a ^{57}Co/Rh source and an Oxford cryostat operating in the 4.2−250 K temperature range. Samples for Mössbauer spectroscopy were prepared by grinding crystals in liquid nitrogen. To satisfactorily account for the observed relaxation effects, a simple model was adopted for the case of the sextet, considering the following parameters: the quadruple interaction $\varepsilon = \Delta E_Q (3 \cos^2 \vartheta - 1)$, where ΔE_Q is the limiting quadruple splitting expected under rapid relaxation conditions, and ϑ is the angle between V_{zz} and the hyperfine magnetic field H_{int}.

Electrochemical measurements were carried out with a model PGSTAT30 potentiostat-galvanostat from Autolab Electrochemical Instruments. The entire system was under computer control and supported by the appropriate computer software GPES, running on Windows XP. The electrochemical cell used had platinum (disk) working and auxiliary (wire) electrodes. A Ag/AgCl electrode was used as reference electrode. Thus, the derived potentials in the cyclic voltammetric measurements are referenced to that electrode. The water used in the electrochemical measurements was of nanopure quality. KNO_3 was used as a supporting electrolyte. Normal concentrations used were 1−6 mM in electroanalyte and 0.1 M in supporting electrolyte. Purified argon was used to purge the solutions prior to the electrochemical measurements.

pH-Potentiometric Measurements. The protonation constants of quinic acid were determined by pH-potentiometric titrations of 30 mL samples in the pH range 2.8−11.4, under a purified argon atmosphere. The concentration of quinic acid was in the range of 1.3−5.0 mmol·dm^{-3}. The stability constants of the Fe(III) complexes of quinic acid were determined by pH-potentiometric titrations of 30 mL samples in the pH range 2.3−11.2, under a purified argon atmosphere. All solutions were prepared using Fluka reagent grade D-(-)-quinic acid, $Fe(NO_3)_3 \cdot 9H_2O$, and ultrapure deionized water. To avoid metal hydroxo-polymerization,[8] aqueous solutions of Fe(III) were prepared in HNO_3 (C 10^{-2} mol·dm^{-3}). The purity of quinic acid as well as the exact concentration of

(1) Braun, V.; Hantke, K.; Köster, W. In *Metal Ions in Biological Systems*; Sigel, H., Sigel, A., Eds.; Marcel Dekker, Inc.: New York, 1998; pp 67−145.
(2) (a) Fett, J. P.; LeVier, K.; Guerinot, M. L. In *Metal Ions in Biological Systems*; Sigel, H., Sigel, A., Eds.; Marcel Dekker, Inc.: New York, 1998; pp 187−214. (b) Mori, S. In *Metal Ions in Biological Systems*; Sigel, H.; Sigel, A., Eds.; Marcel Dekker, Inc.: New York, 1998; pp 215−238. (c) Jones, D. L.; Darrah, P. R.; Kochian, L. V. *Plant Soil* **1996**, *180*, 57–66. (d) Guerinot, M. L.; Yi, Y. *Plant Physiol.* **1994**, *104*, 815–820.
(3) (a) Stojiljkovic, I.; Hantke, K. *EMBO J.* **1992**, *11*, 4359–4367.
(4) (a) Springer, B. A.; Sligar, S. G.; Olsen, J. S.; Philips, G. N. *Chem. Rev.* **1994**, *94*, 699. (b) Gerber, N. C.; Sligar, S. G. *J. Am. Chem. Soc.* **1992**, *114*, 8742.
(5) (a) Haslam, E. *Shikimic Acid: Metabolism and Metabolites*; Wiley & Sons: New York, 1993. (b) Pittard, A. J. In *Escherichia coli and Salmonella: Cellular and Molecular Biology*; Neidhardt, F. C., Ed.; ASM Press: Washington, DC, 1996; Chapter 28.
(6) Nguyen, Q. L.; Olmstead, L.; Bains, S.; Franz, A. H. *Arkivoc* **2007**, *9*, 235–251.
(7) Bentley, R. *Crit. Rev. Biochem. Mol. Biol.* **1990**, *25*, 307–384.
(8) Gumienna-Kontecka, E.; Silvagni, R.; Lipinski, R.; Lecouvey, M.; Marincola, F. C.; Crisponi, G.; Nurchi, V. M.; Leroux, Y.; Kozlowski, H. *Inorg. Chim. Acta* **2002**, *339*, 111–118.

quinate and Fe(III) solutions were determined by the Gran method.[9] The exact concentration of Fe(III) was checked by EDTA complexometric titration in the presence of ammonium acetate buffer to give a pH of ~ 2.5 with Variamine Blue B (0.1% solution) as indicator.[10]

The ionic strength of the investigated solutions was adjusted to 0.15 M with NaCl. The temperature was maintained at 25.0 ± 0.1 °C during the measurements. The titrations were carried out with a carbonate-free NaOH solution of known concentration (ca. 0.15 M). The NaOH solution was standardized using potassium hydrogen iodate ($KH(IO_3)_2$). The iron concentration was 1.0 mM, and the employed metal/ligand ratios were 1:3, 1:4, and 1:5. The pH was measured with a computer-controlled Crison titration system, elaborated for titrations at such low concentrations,[11] and a Mettler Toledo-Inlab 412 combined glass-electrode, calibrated for hydrogen ion concentration according to Irving et al.,[12] by using the GLEE program.[13] The ionic product of water was found to be pK_w = 13.76.

The one step protonation constants of quinic acid are given as log K_1, consistent with the equilibrium $L^- + H^+ \rightleftarrows HL$, where $K_1 = [HL]/[L^-][H^+]$. The stepwise protonation constants of quinic acid are given as log K_n, consistent with the equilibrium

$$H_{n-1}L + H \rightleftarrows H_nL \quad \text{where} \quad K_n = [H_nL]/[H_{n-1}L][H]$$

The initial computations were obtained in the form of overall protonation constants $\beta_n = [H_nL]/[L][H]^n$, taking into account that $\beta_n = \prod_n K_n$.

The concentration stability constants $\beta_{pqr} = [M_pL_qH_r]/[M]^p[L]^q[H]^r$ for quinic acid were calculated with Superquad.[14] The corresponding β_{pqr} values for Fe(III)-quinate complexes, formed in the investigated system, were calculated with the PSEQUAD computer program.[15] The pH-dependent species distribution curves and simulated titration curves were obtained from the measured overall formation constants with the HySS program.[16]

The formation of hydroxo complexes of Fe(III) was taken into account in the employed calculations. For these calculations, the fact that ferric ions form several hydrolytic species in aqueous solution was taken into account. To that end, it should be noted that there is a disagreement on the subject of their values in the literature. The stability constants used for the hydroxo species of Fe(III) were taken from data of Lacour et al.,[17] and corrected to I = 0.15 M using the Davies equation:[18] $[FeH_{-1}]^{2+}$ (log $\beta_{1-1} = -2.67$), $[FeH_{-2}]^{+}$ (log $\beta_{1-2} = -6.49$), $[Fe_2H_{-2}]^{4+}$ (log $\beta_{2-2} = -3.09$), $[FeH_{-3}]^{0}$ (log $\beta_{1-3} = -12.94$), and $[FeH_{-4}]^{-}$ (log $\beta_{1-4} = -22.49$).

Preparation of Complex $K[Fe(C_7H_{11}O_6)_3]\cdot(OH)\cdot 3H_2O$ (1). A quantity of $FeCl_3\cdot 6H_2O$ (0.50 g, 1.8 mmol) was placed in a flask and dissolved in 3 mL of H_2O. To that solution, D-(-)-quinic acid (1.1 g, 5.5 mmol) was added slowly and under continuous stirring. KOH was then added slowly to adjust the pH to a final value of ~3. The resulting reaction solution was stirred for 1 h at room temperature. The color of the solution was yellowish and stayed as such. Subsequently, ethanol was added, and the reaction mixture was placed at 4 °C. A few days later, yellowish cubic crystals appeared at the bottom of the flask. The crystals were isolated by filtration and dried in vacuo. The yield was 1.0 g (72%). Anal. Calcd for **1**, $K[Fe(C_7H_{11}O_6)_3]\cdot(OH)\cdot 3H_2O$, M.W. 739.48: C, 34.08; H, 5.40; Found: C, 34.03; H, 5.50.

Preparation of Complex $(NH_4)[Fe(C_7H_{11}O_6)_3]\cdot(OH)$ (2). A quantity of $FeCl_3\cdot 6H_2O$ (0.50 g, 1.8 mmol) was placed in a flask and dissolved in 3 mL of H_2O. To that solution, D-(-)quinic acid (1.1 g, 5.5 mmol) was added slowly and under continuous stirring. Aqueous ammonia was then added slowly to adjust the pH to a final value of ~3.5. The resulting reaction solution was stirred for 1 h at room temperature. The color of the solution was yellowish and stayed as such. Subsequently, ethanol was added, and the reaction mixture was placed at 4 °C. A few days later, yellowish crystals appeared at the bottom of the flask. The crystals were isolated by filtration and dried in vacuo. The yield was 0.75 g (~56%). Anal. Calcd for **2**, $(NH_4)[Fe(C_7H_{11}O_6)_3]\cdot(OH)$ M.W. 664.37: C, 37.93; H, 5.72; N, 2.11; Found: C, 37.50; H, 5.80; N, 2.10.

Preparation of Complex $Na[Fe(C_7H_{11}O_6)_3]\cdot(OH)\cdot 8H_2O$ (3). A quantity of $FeCl_3\cdot 6H_2O$ (0.50 g, 1.8 mmol) was placed in a flask and dissolved in 3 mL of H_2O. To that solution, D-(-)quinic acid (1.1 g, 5.5 mmol) was added slowly and under continuous stirring. Aqueous sodium hydroxide solution was then added slowly to adjust the pH to a final value of ~3.5. The resulting reaction solution was stirred for 1 h at room temperature. The color of the solution was yellowish and stayed as such. The resulting reaction mixture was allowed to stand at room temperature. Two months later, yellowish crystals appeared at the bottom of the flask upon slow evaporation. The crystals were isolated by filtration and dried in vacuo. The yield was 0.75 g (~56%). Anal. Calcd for **3**, $Na[Fe(C_7H_{11}O_6)_3]\cdot(OH)\cdot 8H_2O$ M.W. 813.45: C, 30.97; H, 6.15. Found: C, 30.18; H, 5.96.

X-ray Crystallography

Crystal Structure Determination. X-ray quality crystals of compounds **1** and **2** were grown from water-ethanol reaction mixtures. Single crystals of **3** were grown from the reaction mixtures upon slow evaporation. A single crystal with dimensions 0.25 × 0.21 × 0.15 mm (**1**), 0.25 × 0.19 × 0.16 mm (**2**), and 0.31 × 0.26 × 0.22 mm (**3**) was mounted on the tip of a glass fiber with epoxy glue. X-ray diffraction data were collected on a Bruker AXS SMART 1K CCD area detector, with graphite monochromated Mo Kα radiation (λ = 0.71073 Å), at room temperature using the program SMART-NT.[19] The collected data were processed by SAINT-NT.[20] An empirical absorption correction was applied by the program SADABS.[20] The structures were solved by direct methods and refined by full-matrix least-squares methods on F^2.[21] In all structures (**1**, **2**, and **3**), all non-hydrogen atoms were refined anisotropically. Hydrogen atoms on carbon atoms were geometrically positioned and

(9) (a) Gran, G. *Acta Chem. Scand.* **1950**, *29*, 559. (b) Gran, G. *Analyst* **1952**, *77*, 661–671. (c) Rossotti, F. J. C.; Rossotti, H. *J. Chem. Educ.* **1965**, *42*, 375–378.
(10) Cohen, S. M.; O'Sullivan, B.; Raymond, K. N. *Inorg. Chem.* **2000**, *39*, 4339–4346.
(11) Pettit, L. D. *Molspin pH-meter Instruction Manual*; Molspin Ltd.: England.
(12) Irving, H. M.; Miles, M. G.; Petit, L. D. *Anal. Chim. Acta* **1967**, *38*, 475–479.
(13) Gans, P.; O'Sullivan, B. *Talanta* **2000**, *51*, 33–37.
(14) Gans, P.; Sabatini, A.; Vacca, A. *J. Chem. Soc., Dalton Trans.* **1985**, 1195.
(15) Zékány, L.; Nagypál, I.; Peintler, G. *PSEQUAD for Chemical Equilibria*; Technical Software Distributions: Baltimore, 1991.
(16) Alderighi, L.; Gans, P.; Ienco, A.; Peters, D.; Sabatini, A.; Vacca, A. *Coord. Chem. Rev.* **1999**, *184*, 311–318.
(17) Lacour, S.; Deluchat, V.; Bollinger, J.-C.; Serpaud, B. *Talanta* **1998**, *46*, 999–1009.
(18) Colston, B. J.; Robinson, V. J. *Analyst* **1997**, *122*, 1451–1455.
(19) *SMART-NT*, Version 5.0; Brucker AXS: Madison, WI, 1998.
(20) *SAINT-NT*, Version 5/6.0;Brucker AXS: Madison, WI, 1999.
(21) *SHELXTL-NT*, Version 5.1; Brucker AXS: Madison, WI, 1998.

Table 1. Summary of Crystal, Intensity Collection and Refinement Data for $K[Fe(C_7H_{11}O_6)_3]\cdot(OH)\cdot 3H_2O$ (**1**), $(NH_4)[Fe(C_7H_{11}O_6)_3]\cdot(OH)$ (**2**), and $Na[Fe(C_7H_{11}O_6)_3]\cdot(OH)\cdot 8H_2O$ (**3**)

	1	**2**	**3**
formula	$C_{21}H_{40}FeKO_{22}$	$C_{21}H_{38}FeNO_{19}$	$C_{21}H_{50}FeNaO_{27}$
formula weight	739.48	664.37	813.45
temperature, °K	293(2)	298(2)	303(2)
wavelength	Mo Kα 0.71073	Mo Kα 0.71073	Mo Kα 0.71073
space group	$P2_13$	$P2_13$	$P2_13$
a (Å)	15.1693(9)	15.2831(9)	15.6019(14)
b (Å)	15.1693(9)	15.2831(9)	15.6019(14)
c (Å)	15.1693(9)	15.2831(9)	15.6019(14)
V, (Å^3)	3490.6(4)	3569.7(4)	3797.8(6)
$a = \beta = \gamma$ (deg)	90.00	90.00	90.00
Z	4	4	4
D_{calcd}/D_{measd} (Mg m^{-3})	1.407/1.41	1.236/1.25	1.423/1.45
abs. coeff. (μ), mm^{-1}	0.633	0.492	0.501
range of h, k, l	$-14 \le h \le 18$	$-20 \le h \le 20$	$-20 \le h \le 20$
	$-18 \le k \le 18$	$-19 \le k \le 13$	$-19 \le k \le 20$
	$-18 \le l \le 18$	$-19 \le l \le 18$	$-13 \le l \le 20$
goodness-of-fit on F^2	1.094	1.139	1.247
R^a	$R = 0.0385^b$	$R = 0.0660^b$	$R = 0.0967^b$
$R_w{}^a$	$R_w = 0.1134^b$	$R_w = 0.1880^b$	$R_w = 0.2740^b$

[a] R values are based on F values, R_w values are based on F^2; $R = \sum||F_o|-|F_c||/\sum(|F_o|)$, $R_w = \{\sum[w(F_o^2 - F_c^2)^2] / \sum[w(F_o^2)^2]\}^{1/2}$; $w = 1/[\sigma^2(F_o^2) + (aP)^2 + bP]$ where $P = (\text{Max}(F_o^2,0) + 2F_c^2)/3$. [b] For 2218 (**1**), 2322 (**2**), and 2706 (**3**) reflections with $I > 2\sigma(I)$.

were left riding on their parent atoms during structure refinement. Hydrogen atom positions, which belong to oxygen atoms, were first determined from E-maps, brought to reasonable distances from their parent oxygen atoms, and then fixed. Hydrogens of lattice water molecules in **3** were not included in the final refined structural model. The oxygen atoms of water molecules and OH^- ions were left in their nascent form. The final assignment satisfies the electroneutrality of compounds **1**, **2**, and **3**, with the understanding that all iron atoms are formally in the oxidation number +3. Crystallographic details for **1**, **2**, and **3** are summarized in Table 1. Further details on the crystallographic studies, as well as atomic displacement parameters, are given as Supporting Information in the form of cif files. Further crystallographic details for **1**: $2\theta_{max} = 52.0°$; reflections collected/unique/used, 20981/2311[R(int) = 0.0309]/2218; 151 parameters refined; $[\Delta\rho]_{max}/[\Delta\rho]_{min}$ = 0.830/−0.327 e/Å^3; R/R_w (for all data), 0.0402/0.1150. For **2**: $2\theta_{max} = 55.9°$; reflections collected/unique/used, 23057/2793 [R(int) = 0.0369]/2322; 136 parameters refined; $[\Delta\rho]_{max}/[\Delta\rho]_{min}$ = 1.251/-0.426 e/Å^3; R/R_w (for all data), 0.0819/0.2015. For **3**: $2\theta_{max} = 56.7°$; reflections collected/unique/used, 26184/3092[R(int) = 0.0452]/2706; 151 parameters refined; $[\Delta\rho]_{max}/[\Delta\rho]_{min}$ = 1.700/−1.045 e/Å^3; R/R_w (for all data), 0.1063/0.2827.

Synthesis. The synthesis of compounds **1**−**3** was pursued through a facile reaction between Fe(III) and quinic acid in aqueous media. The optimal pH, at which the reactions were developed, was in the range 3−3.5. The adjustment of pH was achieved through addition of KOH (**1**), ammonia (**2**), and NaOH (**3**). The general stoichiometric reaction leading to the formation of compounds **1**−**3** in Scheme 1.

The compounds were easily isolated in pure crystalline form upon slow evaporation at room temperature or addition of alcohol to the reaction mixture at 4 °C over a period of a week. Elemental analyses of the isolated crystalline

Scheme 1

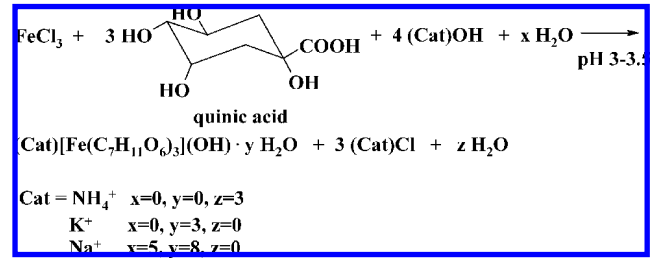

materials suggested the molecular formulation $K[Fe(C_7H_{11}O_6)_3]\cdot(OH)\cdot 3H_2O$ for **1**, $(NH_4)[Fe(C_7H_{11}O_6)_3]\cdot(OH)$ for **2**, and $Na[Fe(C_7H_{11}O_6)_3]\cdot(OH)\cdot 8H_2O$ for **3**, respectively. Attempts to quantitatively identify and account for stoichiometrically present chloride ions in the lattice of the derived species showed only spurious amounts. It appears that the use of ammonia, NaOH, and KOH as bases, usually added to raise the pH of the reaction mixture, led to their incorporation into the corresponding lattices of **1**, **2**, and **3**. Further spectroscopic evaluation of **1**−**3** by FT-IR confirmed the presence of quinate bound to Fe(III), thus lending credence to the proposed formulation. Efforts were also made to pursue the synthesis and isolation of species under identical conditions of molecular stoichiometry of Fe(III): quinate, at higher pH values reaching up to 7. In all of those cases, the ultimately isolated crystalline product was identical to that of **1**−**3**, but the yield was lower. The identity of the crystalline products **1**−**3** isolated in the extended pH range was proven through (a) FT-IR spectroscopy, and (b) X-ray cell determination of single crystals of the respective compounds.

All three compounds **1**−**3** were insoluble in organic solvents, methanol, ethanol, acetonitrile, chlorinated solvents ($CHCl_3$, CH_2Cl_2), toluene, and DMF. They were all stable in the air at room temperature for long periods of time.

X-ray Crystallographic Structures. The X-ray crystal structure of **1**−**3** reveals the presence of discrete species $[Fe(C_7H_{11}O_6)_3]$, with accompanying cations and OH^- anions in the lattice. The Oak Ridge Thermal Ellipsoid Plot (ORTEP) diagram for complex **1** is shown in Figure 1, while a packing view of complex **2** is provided in Figure 2A. A list of selected bond distances and angles for **1**−**3** are given in Table 2. Complexes **1**−**3** crystallize in the cubic crystal system and in the space group $P2_13$, with four molecules per unit cell. In all three cases, the metal-quinate assembly is the same from the coordination point of view. The structures show a mononuclear complex of Fe(III) with three quinate ligands coordinated to it. In all three complexes, each quinate acts as a bidentate ligand with the alcoholic (O1) and carboxyl (O5) oxygens coordinated to Fe(III). The quinate ligands are singly deprotonated, with the deprotonated site being the carboxylate group. The α-hydroxy group remains protonated and as such it coordinates to the metal ion center.

A similar case of a α-hydroxycarboxylate-metal complex with bound citrates had been previously observed in the case of Al(III) and Ga(III). Specifically, the complexes $(NH_4)_4[Al(C_6H_4O_7)(C_6H_5O_7)]\cdot 3H_2O$[22] and $(NH_4)_4[Ga(C_6H_4O_7)(C_6H_5O_7)]\cdot 3H_2O$[22] contained a similar coordination en-

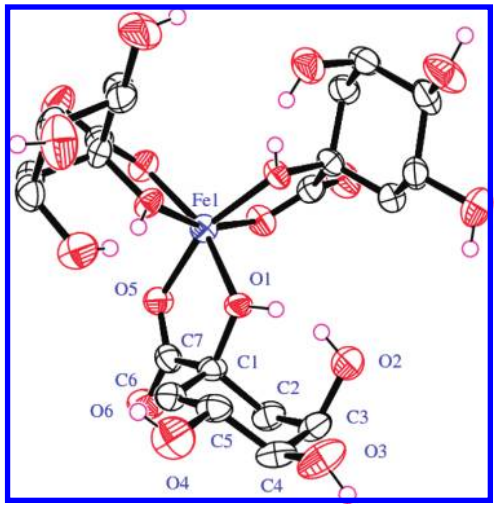

Figure 1. ORTEP structure of $[Fe(C_7H_{11}O_6)_3]$ (**1**) with the atom labeling scheme. Thermal ellipsoids are drawn by ORTEP and represent 50% probability surfaces.

vironment generated by two citrate ligands differing in their deprotonation state. The fact that the α-alcoholic group is protonated stands in contrast to the corresponding alcoholic group in the citrate ligand bound to M(III) in $[M(C_6H_4O_7)_2]^{5-}$ (M = Fe(III), Mn(III)). There, despite the presence of a α-hydroxycarboxylate moiety being present in the citric acid ligand, the alcoholic group was deprotonated upon coordination to the M(III) ion.

The Fe−O bond distances in **1**−**3** compare favorably with those observed in the crystal structure of the complexes $(NH_4)_5[Fe(C_6H_4O_7)_2]\cdot 2H_2O$ (1.953(2)−2.068(2) Å) (**4**),[23] $(Hpy)_2[Fe_2(C_6H_6O_7)_2(H_2O)_2]\cdot 2H_2O$ (1.987(3)−2.038(3) Å) (**5**), $(Hneo)_3[Fe_2(C_6H_5O_7)_3]\cdot nH_2O$ (1.938(3)−2.068(3) Å) (**6**),[24] $(Hneo)_7[Fe_9O(C_6H_6O_7)_8(H_2O)_3]\cdot neo\cdot xH_2O$ (1.92(2)−2.22(2) Å) (**7**),[25] $K_3Fe(C_2O_4)_3\cdot 3H_2O$ (1.978(7) and 2.002(7) Å) (**8**),[26] (bipyH) $[Fe(C_2O_4)_2(H_2O)]\cdot H_2O$ (1.962(2)−2.039(2) Å) (**9**),[27] and are in the range of those observed (2.085−2.178(2) Å) in $[Fe(H_2O)_6][Fe(C_6H_5O_7)(H_2O)]_2\cdot 2H_2O$ (**10**),[28] as well as in the quinate complexes $[Zn(C_7H_{11}O_6)_2]$,[29] $[Cd(C_7H_{11}O_6)_2]\cdot H_2O$, $[Cu(C_7H_{10}O_6)(H_2O)]_2(H_2O)_2$,[30] $\{[Cu(NO_3)(C_7H_{11}O_6)(H_2O)]\cdot 2H_2O\}_n$, $\{[CuCl(C_7H_{11}O_6)(H_2O)]\cdot H_2O\}_n$,[31] $[Pt(C_6H_{14}N_2)(C_7H_{10}O_6)]$,[32] and the trinuclear $(NH_4)_2\{[V(O)_2]_2[V(O)](\mu\text{-}C_7H_{10}O_6)_2\}\cdot H_2O$.[33] Overall, the quinate ligand plays the role of a bidentate metal chelator, effectively formulating the coordination environment around Fe(III).

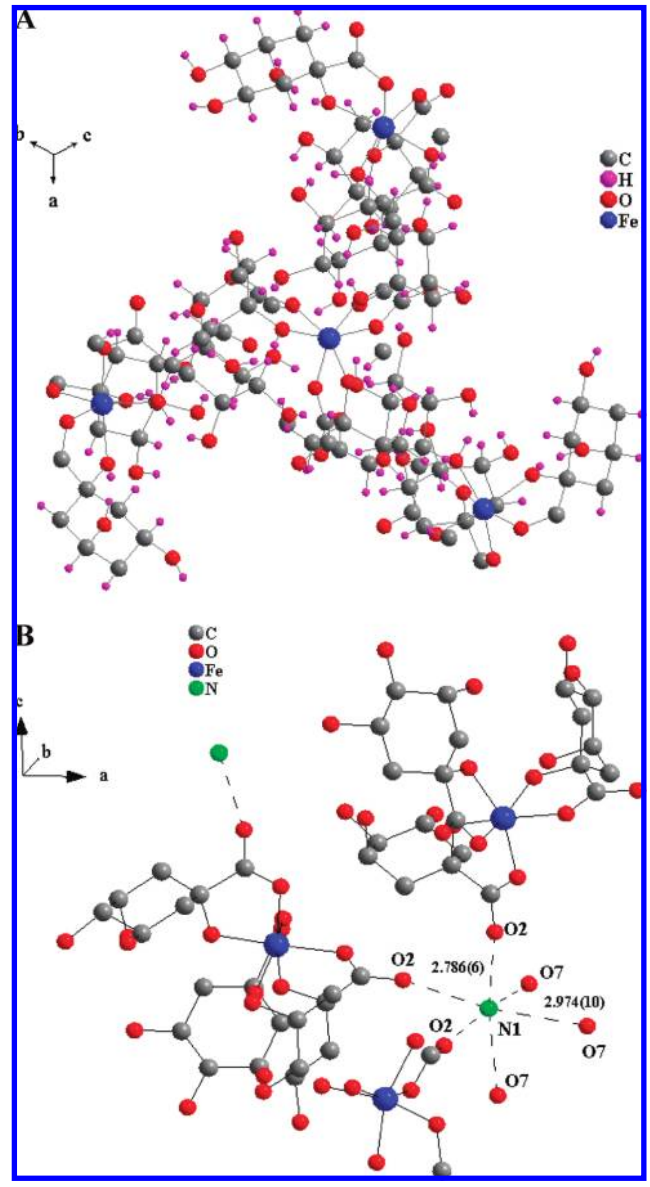

Figure 2. (A) Packing view of complex **2** along the diagonal of the *abc* system. (B) Structure of **2** showing the relationship among the ammonium, quinate and OH^- ions.

The angles are in the range 78.08(8)−105.23(8)° for complex **1**. They are similar to those in complex **2** (78.51(11)−104.91(12)°), **3** (79.09(15)−106.45(17)°), and cover a wide range around the ideal octahedral angle of 90°. The angle values in each case are similar to those observed in (81.86(8)−98.14(8)°) (**4**), (74.60(8)−108.40(9)°), (**7**) and (80.0(1)−94.0(1)°) (**9**) and similar to the quinate organic−inorganic hybrid $[Mn_2(C_7H_{11}O_6)_4]_n\cdot nH_2O$ (69.56(15)−96.75(17)°).[34]

(22) Matzapetakis, M.; Kourgiantakis, M.; Danakali, M.; Raptopoulou, C. P.; Terzis, A.; Lakatos, A.; Kiss, T.; Banyai, I.; Iordanidis, L.; Mavromoustakos, T.; Salifoglou, A. *Inorg. Chem.* **2001**, *40*, 1734–1744.
(23) Matzapetakis, M.; Raptopoulou, C. P.; Tsohos, A.; Papaefthymiou, V.; Moon, N.; Salifoglou, A. *J. Am. Chem. Soc.* **1998**, *120*, 13266–13267.
(24) Shweky, I.; Bino, A.; Goldberg, D. P.; Lippard, S. J. *Inorg. Chem.* **1994**, *33*, 5161–5162.
(25) Bino, A.; Shweky, I.; Cohen, S.; Bauminger, S.; Lippard, S. J. *Inorg. Chem.* **1998**, *37*, 5168–5172.
(26) Delgado, G.; Mora, A. J.; Sagredo, V. *Phys. B* **2002**, *320*, 410.
(27) Decurtins, S.; Schmalle, H. W.; Schneuwly, P.; Oswald, H. R. *Inorg. Chem.* **1993**, *323*, 1888.
(28) Strouse, J.; Layten, S. W.; Strouse, C. E. *J. Am. Chem. Soc.* **1977**, *99*, 562–572.
(29) Inomata, Y.; Haneda, T.; Howell, F. S. *J. Inorg. Biochem.* **1999**, *76*, 13–17.
(30) Barba-Behrens, N.; Salazar-Garcia, F.; Bello-Ramirez, A. M.; Garcia-Baez, E.; Rosales-Hoz, M. J.; Contreras, R.; Flores-Parra, A. *Trans. Met. Chem.* **1994**, *19*, 575.
(31) Bkouche-Walksman, I. *Acta Crystallogr., Sect. C.* **1994**, *50*, 62.
(32) Hata, G.; Kitano, Y.; Kaneko, T.; Kawai, H.; Mutoh, M. *Chem. Pharm. Bull.* **1992**, *40*, 1604.
(33) Codd, R.; Hambley, T. W.; Lay, P. A. *Inorg. Chem.* **1995**, *34*, 877.
(34) Menelaou, M.; Raptopoulou, C. P.; Terzis, A.; Tangoulis, V.; Salifoglou, A. *Eur. J. Inorg. Chem.* **2005**, *10*, 1957–1967.

Table 2. Bond Lengths [Å] and Angles [deg] for **1**, **2**, and **3**

1[a]		**2**[b]		**3**[c]	
		Bond Distances (Å)			
Fe(1)−O(1)	1.998(2)	Fe(1)−O(1)	1.992(2)	Fe(1)−O(1)	1.921(4)
Fe(1)−O(5)	1.992(2)	Fe(1)−O(3)	1.999(3)	Fe(1)−O(2)	2.081(4)
		Angles (deg)			
O(5)−Fe(1)−O(1)	78.08(7)	O(3)−Fe(1)−O(1)	78.51(11)	O(1)−Fe(1)−O(2)‘	79.09(15)
O(5)′−Fe(1)−O(1)	105.23(8)	O(3)′−Fe(1)−O(1)	104.91(12)	O(1)−Fe(1)−O(2)	106.45(17)
O(5)′−Fe(1)−O(5)	91.95(8)	O(3)′−Fe(1)−O(3)	91.27(13)	O(1)−Fe(1)−O(1)′	93.84(16)
O(1)−Fe(1)−O(1)′	88.07(8)	O(1)−Fe(1)−O(1)′	88.49(11)	O(2)−Fe(1)−O(2)′	83.79(16)
O(1)−Fe(1)−O(5)″	160.27(8)	O(1)−Fe(1)−O(3)″	160.91(11)	O(1)−Fe(1)−O(2)″	158.83(16)

[a] Symmetry transformations used to generate equivalent atoms: ′ $-z + 1/2, -x, y + 1/2$; ″ $-y, z - 1/2, -x + 1/2$. [b] Symmetry transformations used to generate equivalent atoms: ′ $y - 1/2, -z + 3/2, -x + 1$; ″ $-z + 1, x + 1/2, -y + 3/2$. [c] Symmetry transformations used to generate equivalent atoms: ′ $-y + 3, z + 1/2, -x + 5/2$; ″ $-z + 5/2, -x + 3, y - 1/2$.

In complex **1**, each potassium ion is in contact with three carboxylate O-atoms from three quinate ligands, as well as bound to three disordered water molecules (O7 and O8). In the same species, each quinate ligand bridges one Fe(III) ion and one potassium ion through the two O atoms of the carboxylate moiety. The distance between K^+ and Fe(III) is 6.725(1) Å. Each Fe(III) is connected via quinate bridges to three K^+ ions, forming an equilateral triangle. Meanwhile, each K^+ ion is located above the center of a Fe_3-triangle (Supporting Information Figure 1), resulting in the formation of an infinite three-dimensional (3D) network (Supporting InformationFigure 2).

In complex **2**, the ammonium counterions replace the potassium cations of complex **1** and the N-atoms are in contact with the carboxylate oxygens (O6) of the quinate anion, as well as bound to OH^- oxygens (O7) through hydrogen-bonding at distances in the range 2.774(7)−2.981(12) Å (Figure 2B). In complex **3**, beyond the eight water molecules of crystallization in the lattice, there exist sodium ions each interacting with three pairs of adjacently located alcoholic oxygens (O4 and O5 from the quinate triol functionalities). Each alcoholic pair belongs to a separate discrete Fe(III)-quinate complex. The sodium, potassium, and ammonium ions in the respective lattices of **1**−**3** help link the assemblies together along with OH^- ions. Consequently, a 3D network of hydrogen bonds forms, which involves quinate hydroxyl oxygens and carboxylate oxygens, as well as OH^- oxygens. The resulting extensive hydrogen-bonding network very likely contributes to the stability of the crystal lattices in **1**−**3**.

UV/vis Spectroscopy. The electronic spectrum of **1** was recorded in H_2O. The spectrum showed bands at 354 nm (ε 1572 M^{-1} cm^{-1}), 334 nm (ε 1587 M^{-1} cm^{-1}), and 229 nm (ε 2652 M^{-1} cm^{-1}), with the latter feature rising well into the ultraviolet region. All three bands have been attributed to the presence of a quinate oxygen to Fe(III) Ligand to Metal Charge Transfer (LMCT). The spectrum was featureless beyond 400 nm.

FT-IR Spectroscopy. The FT-IR spectra of **1**, **2**, and **3** exhibit strong absorptions for the carbonyl carboxylate groups in both the antisymmetric and symmetric vibration regions. The antisymmetric stretching vibrations $\nu_{as}(COO^-)$ appear in the range from 1660 to 1637 cm^{-1} (**1**), 1666 to 1635 cm^{-1} (**2**), and 1642 to 1597 cm^{-1} (**3**), respectively, whereas the corresponding symmetric stretches $\nu_s(COO^-)$ appear in the range from 1385 to 1330 cm^{-1} (**1**), 1400 to 1332 cm^{-1} (**2**), and 1397 to 1345 cm^{-1} (**3**), respectively. The frequencies for the carbonyl stretches in **1**, **2**, and **3** are shifted to lower values in comparison to those of the free quinic acid. From that point of view, they indicate a change in the vibrational status of the quinate anion upon coordination to the metal ion.[35] It specifically suggests that the carboxylate groups of the quinate ligand were either free or coordinated to Fe(III) in a monodentate fashion.[36] Similar trends in the frequencies of the carboxylate carbonyls had been previously observed in the FT-IR spectra of α-hydroxycarboxylate complexes of other trivalent, as well as divalent metal ions.[37]

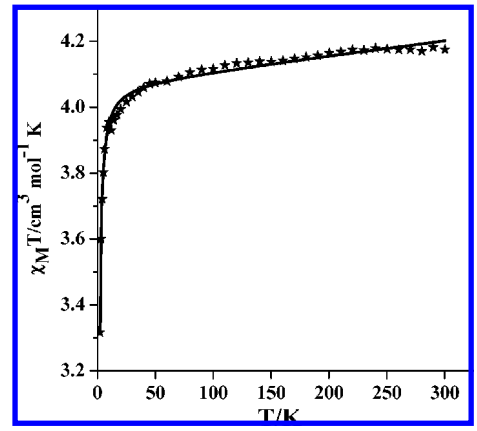

Figure 3. Temperature dependence of the susceptibility data in the form of $\chi_M T$ vs T (solid stars) in the temperature range 2−300 K, and fitting results using the theoretical formula discussed in the text (solid line).

Cyclic Voltammetry. The cyclic voltammetry of complex **2** was studied in aqueous solutions in the presence of KNO_3 as a supporting electrolyte. The cyclic voltammogram projects a ill-defined electrochemical behavior with a pronounced irreversible wave at −0.75 V versus Ag/AgCl or −0.55 V versus NHE ($ip_a/ip_c < 1$, $ip_c/\{(\upsilon)^{1/2}C\}$ variable). This irreversible reduction wave reflects complex process(es) involving the Fe(III)/Fe(II) redox couple. Attempts to pursue the redox chemistry of complex **2** at such low reduction potentials are currently ongoing.

Magnetic Susceptibility Studies. The temperature dependence of $\chi_M T$ (χ_M being the magnetic susceptibility for one Fe(III) ion) for complex **1** is shown in Figure 3 (solid stars). The $\chi_M T$ value is 4.17 cm^3 mol^{-1} K at 300 K, close to the value expected for an isolated ion of Fe(III), which is 4.38 cm^3 mol^{-1} K. From 300 K down to 10 K, there is a

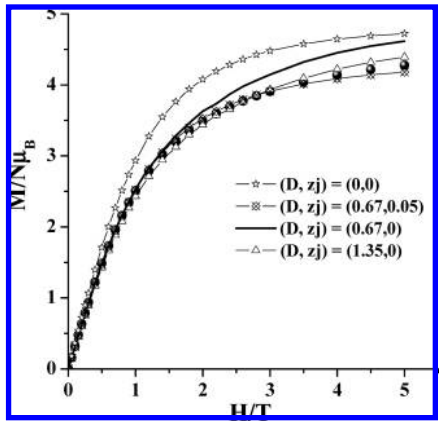

Figure 4. Magnetization measurements in the field range 0−5 T and at temperature $T = 2$ K (solid cycles). The fitting results are obtained using different theoretical models discussed in the text.

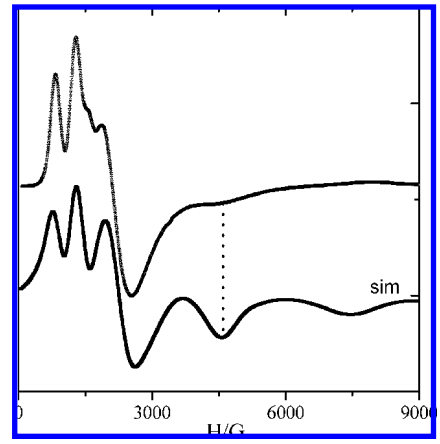

Figure 5. Experimental X-Band EPR powder spectra (microwave resonance 9.61 GHz) of complex **1** at 4 K, and the simulated spectrum according to the theoretical model discussed in the text.

smooth linear decrease, while below that temperature and toward 2 K, a more pronounced decrease is observed, reaching the value of 3.3 $cm^3\ mol^{-1}$ K. The shape of this curve is characteristic of the occurrence of zero field effects. The susceptibility data were fitted by the following equation:

$$H = D\left[S_z^2 - \frac{1}{3}S(S+1)\right] + E(S_x^2 - S_y^2) + g_z\mu_B H_z S_z + g_x\mu_B H_x S_x + g_y\mu_B H_y S_y \quad (1)$$

where an anisotropic g-value ($g_{||}$, $g_{\perp}$)[38] was used. The best fit (solid line in Figure 3) is given by the parameters $D = 0.31(4)$ cm^{-1} and ($g_{||}$, $g_{\perp}$) = (2.16, 1.95).

Isothermal magnetization curves at $T = 2$ K in an applied field range of 0−5 T are shown in Figure 4. The Brillouin function of an uncorrelated spin $S = 5/2$ with the g values obtained from the susceptibility data is shown in the same figure as a line and open stars. The discrepancy between the theoretical and the experimental curve (solid circles) is mainly due to the fact that intermolecular interactions and/or zero-field effects are important in this low temperature regime.

A different magnetic model was used to fit the magnetization data according to the following modified Hamiltonian:

$$H = D\left[S_z^2 - \frac{1}{3}S(S+1)\right] + E(S_x^2 - S_y^2) + g_z\mu_B H_z S_z + g_x\mu_B H_x S_x + g_y\mu_B H_y S_y - zJ\langle S_z\rangle S_z \quad (2)$$

where the g values were fixed or allowed to vary in the vicinity of the values obtained from the susceptibility data for overparameterization reasons. Also, the E parameter was not included in the fitting attempts because of the obvious correlation with the D parameter. The results are also shown in the same figure. When the intermolecular interactions are set to zero (zj = 0) and the only fitted parameter is the zero-field parameter (D), then the resulting value, 1.35 cm^{-1}, is very high in comparison to the fitting results of the susceptibility data (line and open triangles). When the D parameter is set to zero and the only fitted parameter is the intermolecular interaction, then the resulting value, 0.35 cm^{-1}, is unrealistically high (not shown in the Figure). When both parameters are allowed to vary, the emerging results seem to be acceptable since the zero-field parameter D has the same value as before, 0.67 cm^{-1}, and the mean field correction is small, zj = 0.05 cm^{-1}. To see the influence of the mean field correction, the magnetization curve with $D = 0.67$ cm^{-1} and zj = 0 is also shown in the same figure (solid line).

EPR Spectroscopy. X-Band EPR measurements were carried out in powder samples of **1**, as well as in frozen solutions of it in water, and are shown in Figure 5 and 6, respectively. The system does not retain its structure in solution, where a typical rhombic signal $g = 4.3$ signal appears as it is clearly shown in Figure 6. The powder spectrum at helium temperature was simulated with eq 1 for a spin $S = 5/2$, and the simulated spectra are shown in Figure 5.

An isotropic magnetic-field domain line width was used for the powder spectrum (lw = 28 G), with the broadness of the spectrum revealing the presence of g-strain effects. Gaussian distributions of the g-principal values were used, and the results are $\sigma g_x = \sigma g_y = 0.1$, $\sigma g_z = 0.2$. The principal g values for the powder spectrum are $g_{xy} = 1.98(1)$, $g_z = 1.98(1)$. The value of the zero-field parameter D is 0.21(2) cm^{-1} and that of $\lambda = E/D = 0.15(1)$, revealing the rhombic character of the system. Gaussian distributions of the D and E parameters were also used ($\sigma(D) = 0.03$, $\sigma(E) = 0.04$). The correctness of the model is verified by the reproduction of weak and broad peaks (depicted with stars in the experimental spectrum). The correctness of the model is verified by the reproduction of weak and broad peaks (depicted with stars in the experimental spectrum).

The discrepancy between the EPR results and the magnetic susceptibility studies concerning the value of the D parameter emerges mainly from sensitivity reasons. With regard to the magnetic fitting procedure, it would be necessary to measure the entire "magnetic space", that is the 3D space defined by temperature, the external magnetic field, and the resulting magnetization. In the measurements presented here, we only have two sections in this space, namely, variable-temperature susceptibility at one fixed field and variable-field magnetization at one fixed temperature.

Mössbauer Spectroscopy. Zero-field Mössbauer spectra of polycrystalline samples of **1**were recorded in the 4.2−250 K temperature range. Representative spectra are shown in Figure 7. At high temperatures, the spectrum consists of a relatively broad single line at ∼0 mms^{-1}. This behavior indicates strongly the presence of relaxation effects[39] and such spectra are frequently observed in mononuclear high-spin ferric complexes.[40] As the temperature decreases, the central line becomes broader, and for $T < 100$ K a magnetically split spectrum (a sextet) emerges. At 4.2 K, the sextet lines are better defined, however, they still remain relatively broad. In the temperature range 4.2−100 K, the behavior of the sextet is more consistent with a paramagnetic relaxation rather than a long-range ordering (LRO), in agreement with the magnetic susceptibility measurements, in which no evidence for LRO was found for the investigated temperature range.

To effectively account for the relaxation effects, we have adopted a simple model[41] for the case of the sextet. For that model, we assume that the internal magnetic field flips randomly between two values $+H_{int}$ and $-H_{int}$ within a characteristic time T_S. The obtained parameters are isomer shift, $\delta = 0.49(2)$ mms^{-1}; quadruple interaction, $\varepsilon = +0.30(4)$ mms^{-1}; hyperfine field, $H_{int} = 53(2)$ T. The characteristic time T_S for the spin fluctuations is of the order of $2-3 \times 10^{-7}$ s at 4.2 and 78 K, and apparently faster at higher temperatures. The values of δ and H_{int} are consistent with Fe(III) ($S = 5/2$) in an O_6 environment. The non-zero value of quadruple splitting indicates deviations from cubic symmetry.

The zero-field Mössbauer spectra recorded below 100 K consist of two different species as far as the relaxation behavior is concerned. One species gives rise to a sextet, which corresponds to long relaxation times. The second species corresponds to a single broad line at about 0 mms^{-1} and suggests faster relaxation times. From the magnetic susceptibility measurements and EPR spectroscopy, it appears that the magnetic properties of **1** are governed by the

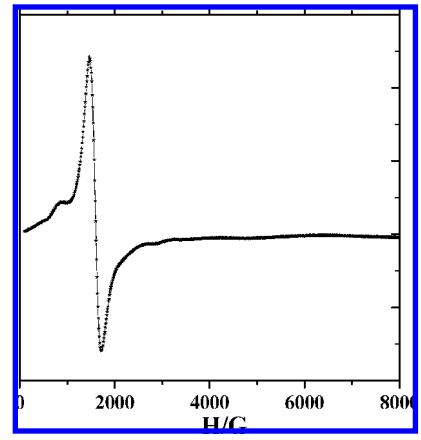

Figure 6. Experimental X-Band EPR solution spectrum of complex **1** (microwave resonance 9.43 GHz) at 4 K.

$S = 5/2$ spin Hamiltonian of equation 1 with a zero field splitting, D, of the order of $0.2-0.8$ cm^{-1}. Because of the D term, the 6-fold degeneracy of the $S = 5/2$ system is partially lifted at zero field, yielding three Kramers' doublets $|\pm 1/2\rangle$, $|\pm 3/2\rangle$, and $|\pm 5/2\rangle$. The separation between the $|\pm 1/2\rangle$ doublet and the $|\pm 3/2\rangle$, and $|\pm 5/2\rangle$ ones is $\sim 2|D|$ and $\sim 6|D|$, respectively. For a Fe(III) ($S = 5/2$) ion, it is well-known that the three Kramers' doublets have different relaxation properties; [42] and the $|\pm 5/2\rangle$ doublet exhibits the longest relaxation times.

A possible interpretation of the Mössbauer spectra for **1** is that the sextet observed for temperatures $T < 100$ K arises from the $|\pm 5/2\rangle$ doublet (with long relaxation times), whereas the broad central line originates from the other two (with shorter relaxation times, even at 4.2 K). Within this model, the coexistence of slow and fast-relaxing spectra at 4.2 K implies that, at this temperature, the three doublets are appreciably populated. This may occur for a relatively small energy separation between the doublets ($|D| < 1$ cm^{-1}), a result effectively in agreement with the findings of the magnetic susceptibility measurements and EPR spectroscopy. Moreover, approximate simulations suggest that the area corresponding to the sextet is larger in the 4.2 K spectrum (ca. 45%) than that in the spectrum at 78 K (ca. 34%), essentially implying that the $|\pm 5/2\rangle$ doublet is the ground state of the system and hence a negative sign for D.

Speciation Studies. Potentiometric titrations of (a) the ligand quinic acid alone, and (b) Fe(III) with D-(-)-quinic acid in various metal ion to ligand molar ratios were carried out. Some of the obtained titration curves, both experimental and calculated, are shown in Figure 8. The titration curves were evaluated with various potential speciation models. The best fit between the experimental and calculated titration curves for the binary Fe(III)-quinic acid system was obtained by considering the mononuclear species $[FeLH_{-1}]^+$, $[FeL_2H_{-1}]^0$ at low pH, the dinuclear forms $[Fe_2L_3H_{-4}]^-$, $[Fe_2L_3H_{-5}]^{2-}$, and the mononuclear species $[FeLH_{-3}]^-$, $[FeLH_{-4}]^{2-}$ (LH = $C_7H_{12}O_6$, and L = $C_7H_{11}O_6^-$) toward the end of the investigated pH range. The fit was reasonably good in the overall pH and

(35) Deacon, G. B.; Philips, R. *J. Coord. Chem. Rev.* **1980**, *33*, 227–250.
(36) Djordjevic, C.; Lee, M.; Sinn, E. *Inorg. Chem.* **1989**, *28*, 719–723.
(37) (a) Matzapetakis, M.; Raptopoulou, C. P.; Terzis, A.; Lakatos, A.; Kiss, T.; Salifoglou, A. *Inorg. Chem.* **1999**, *38*, 618–619. (b) Matzapetakis, M.; Dakanali, M.; Raptopoulou, C. P.; Tangoulis, V.; Terzis, A.; Moon, N.; Giapintzakis, J.; Salifoglou, A. *J. Biol. Inorg. Chem.* **2000**, *5*, 469–474. (c) Matzapetakis, M.; Karligiano, N.; Bino, A.; Dakanali, M.; Raptopoulou, C. P.; Tangoulis, V.; Terzis, A.; Giapintzakis, J.; Salifoglou, A. *Inorg. Chem.* **2000**, *39*, 4044–4051. (d) Griffith, W. P.; Wickins, T. D. *J. Chem. Soc. A.* **1968**, 397–400. (e) Vuletic, N.; Djordjevic, C. *J. Chem. Soc., Dalton Trans.* **1973**, 1137–1141. (f) Kaliva, M.; Giannadaki, T.; Raptopoulou, C. P.; Tangoulis, V.; Terzis, A.; Salifoglou, A. *Inorg. Chem.* **2001**, *40*, 3711–3718. (g) Tsaramyrsi, M.; Kavousanaki, D.; Raptopoulou, C. P.; Terzis, A.; Salifoglou, A. *Inorg. Chim. Acta* **2001**, *320*, 47–59.
(38) Different theoretical models were used to fit the susceptibility data. (a) The case of an isotropic g-value gave bad fitting results (b) the inclusion of the E-parameter gave large correlations between the D and E parameters with no improvement of the fitting results.
(39) Blume, M.; Tjon, J. A. *Phys. Rev.* **1968**, *165*, 446–456.
(40) (a) Greenwood, N. N.; Gibb, T. C. *Mössbauer Spectroscopy*; Chapman and Hall: London, 1972. (b) Deeney, F. A.; Nelson, S. M. *J. Phys. Chem. Solids* **1973**, *34*, 277–282. (c) Korendovych, I. V.; Staples, R. J.; Reiff, W. M.; Rybakova-Akimova, E. V. *Inorg. Chem.* **2004**, *43*, 3930–3941.
(41) van der Woude, F.; Dekker, A. J. *Phys. Status Solidi* **1965**, *9*, 775–785.
(42) Blume, M. *Phys. Rev. Lett.* **1967**, *18*, 305–308.

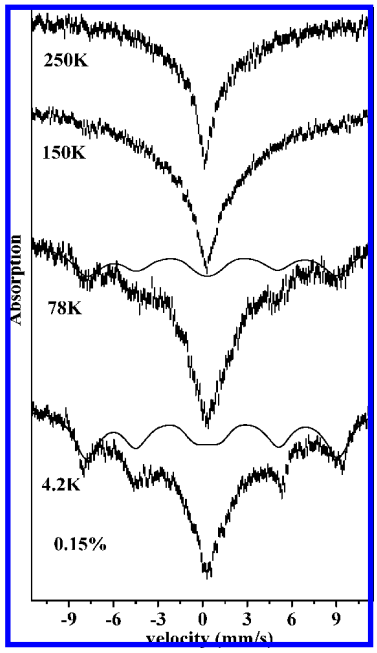

Figure 7. Mössbauer spectra from a polycrystalline sample of **1** recorded at various temperatures as indicated. The solid lines superimposed in the 4.2 and 78 K spectra are theoretical simulations corresponding to the sextet (see text for details).

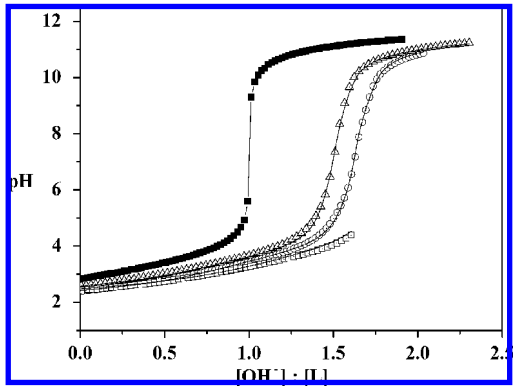

Figure 8. Potentiometric titration curves of free quinic acid (black squares; c_{ligand} = 0.003042 mol dm^{-3}), and Fe(III)−quinic acid with molar ratios 1:3 (squares, c_{Fe} = 0.000967 mol·dm^{-3}, c_{ligand} = 0.003042 mol·dm^{-3}); 1:4 (circles, c_{Fe} = 0.00166 mol·dm^{-3}, c_{ligand} = 0.00663 mol·dm^{-3}); 1:5 (up triangle, c_{Fe} = 0.001 mol·dm^{-3}, c_{ligand} = 0.00498 mol·dm^{-3}). Continuous lines, calculated curves.

concentration range used, demonstrating that the adopted speciation model is satisfactorily defined. Other 1:1 Fe(III):quinate complexes or variably protonated and deprotonated species were rejected by the computer program (PSEQUAD) during the computational process. The species emerging from the speciation distribution of the binary system (Figure 9) are reflected as structural derivative variants of species **1**−**3** synthesized and isolated in the solid state. As such, they indicate that the 3*x*(COO^-, OH) composition in the six coordinate octahedral geometry, observed in the solid state, does not necessarily persist in solution in the whole pH range. The stability constants of the complexes formed are listed in Table 3. The uncertainties (3SD values) of the stability constants are given in parentheses. The pH range of their optimal formation is also reported. For the titratable carboxylate

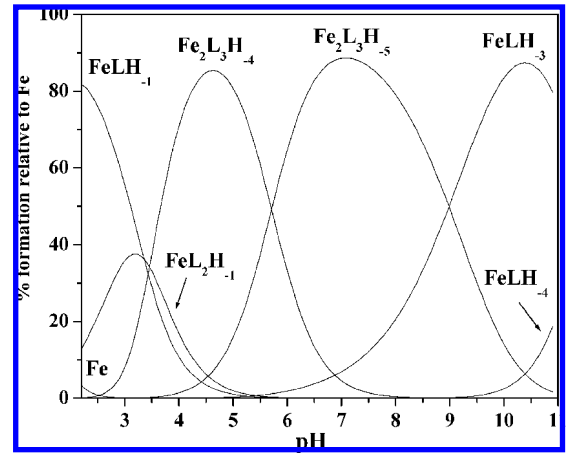

Figure 9. Speciation curves for complexes forming in the Fe(III)−quinic acid system; c_{Fe} = 0.001667 mol·dm^{-3}, c_{ligand} = 0.006635 mol·dm^{-3}. Charges are omitted for clarity.

Table 3. Proton (log *K*) and Fe(III) Complex Formation Constants (log *β*) of Quinic Acid (QA) at *I* = 0.15 (NaCl) and 25°C[a]

	quinic acid	Fe−QA	pH range for each species
log *K*(HL)	3.34(1)		
log *β* ($FeLH_{-1}$)		2.80(5)	<5
log *β* (FeL_2H_{-1})		5.47(4)	<5
log *β* ($FeLH_{-3}$)		−7.83(6)	>6
log *β* ($FeLH_{-4}$)		−19.45(5)	>9.5
log *β* ($Fe_2L_3H_{-4}$)		4.38(8)	2.5−7.5
log *β* ($Fe_2L_3H_{-5}$)		−1.30(8)	4−11
fitting[b]		0.010025	
no. of pts.		266	

[a] Charges from the various species are omitted for clarity. [b] Goodness of fit between the experimental and the calculated titration curves expressed in mL of titrant

group of quinic acid, a pK_a value of 3.34 was obtained and found to be very close to the values reported by Clifford (3.40)[43] and Luethy-Krause et al. (3.36),[44] being almost similar to the pK_a (3.40) of chlorogenic acid (an ester of caffeic and quinic acid). For the congener shikimic acid ((3*R*, 4*S*, 5*R*)-3,4,5-trihydroxy 1-cyclohexanecarboxylic acid) the pK_a value is 4.15.[44] The presence of an alcoholic moiety in a position α- to the carboxylate group of quinic acid is associated with an increase of its acid strength,[45] compared to shikimic acid. Furthermore, the four alcoholic moieties in the structure of quinic acid enhance its acidity in comparison to cyclohexane carboxylic acid (pK_a 4.91).[46]

The titrimetric data were evaluated on the premise that complex formation between Fe(III) and the quinate ligand proceeds through metal ion binding of the deprotonated quinate carboxylate and abutting protonanted alcoholic moieties. The titration curves in the absence and presence of Fe(III) suggest formation of hydroxocomplexes in the entire pH domain.[47] In fact, the enhanced ability of Fe(III)

(43) Clifford, M. *Tea and Coffee Trade J.* **1987**, *159*, 35–39.
(44) Luethy-Krause, B.; Pfenninger, I.; Landolt, W. *Trees* **1990**, *4*, 198–204.
(45) Portanova, R.; Lajunen, L. H. J.; Tolazzi, M.; Piispanen, J. *Pure Appl. Chem.* **2003**, *75*, 495–540.
(46) Blanchard, J.; Boyle, J. O.; Van Wagenen, S. *J. Pharm. Sci.* **2006**, *77*, 548–552.
(47) Serratrice, G.; Galey, J.-B.; Aman, E. S.; Dumats, J. *Eur. J. Inorg. Chem.* **2001**, 471–479.

to coordinate alcoholic/alcoholate groups allows for the formation of mixed hydroxo complexes in the entire pH domain investigated. It is worth noting that chlorogenic and caffeic acid were shown[48] spectrophotometrically to form protonated complexes with Fe(III) at very low pH (1−2.5), but there was no spectrophotometric evidence for a reaction between quinic acid and iron(III).[49] On the basis of the analytical and crystallographic data of this work, the alcoholic group of the quinate ligand retains its proton upon binding to Fe(III) in **1**−**3**. Thus, there is seemingly no expected pH-dependence of the deprotonation of that group and the specific mode of binding to Fe(III) over the investigated pH range. Nevertheless, Fe(III) has been known for its ability to induce deprotonation of the weakly acidic alcoholic-OH group in α-hydroxycarboxylic acids such as citric acid.[50]

The potentiometric titrations of the binary Fe(III)-quinic acid system illustrated in Figure 8 show that from pH 2.3 to about pH 4 ([OH^-]:[L] = 1.5) there is a significant region of interest. In this low pH region, three species coexist, namely, Fe(III), $[FeLH_{-1}]^+$, $[FeL_2H_{-1}]^0$, and $[Fe_2L_3H_{-4}]^-$. The neutral species $[FeL_2H_{-1}]^0$ attains a maximum content of 37% around pH 3 (Figure 9).

The formation constants of species $[FeLH_{-1}]^+$ (log β_{11-1} 2.80) and $[FeL_2H_{-1}]^0$ (log β_{12-1} 5.47) are higher than that of the monohydroxo species $[FeH_{-1})]^{2+}$ (log β_{1-1}= −2.67). This way, what can be rationalized is the emergence of the (a) $[FeLH_{-1}]^+$ species at low pH (<4), reaching a maximum content of 80% around pH 2, and (b) $[FeL_2H_{-1}]^0$ species, with a maximum content of 37% around pH 3 (Figure 9). Concurrently, it needs to be emphasized that the $[Fe(OH)]^{2+}$ species is forming at pH < 5.[51] In this regard, it is less likely for a complex species such as $[FeL]^{2+}$ to appear at these low pH values. The formation constant of the $[FeLH_{-1}]^+$ species (log β_{11-1} 2.80) is similar to that of the Fe(III) complex with lactic acid (2.05) reported at 1.0 M ionic strength.[52] As with the Fe(III)-quinate system, a similar type of mononulear species were proposed upon complexation of Fe(III) with citrate.[50]

From the aqueous speciation scheme it could be observed (Figure 9) that the 1:1 and 1:2 Fe(III):quinate stoichiometry is present for the majority of the species. In both stoichiometries of Fe(III):quinate, the binding mode of the quinate ligand could be either through the carboxylate group or through the carboxylate and α- alcoholate groups, while the remaining polyols do not enter the coordination sphere of Fe(III). In fact, chelate coordination of α-hydroxycarboxylate-containing ligands to Fe(III) through carboxylate groups is preferred in other divalent or trivalent metal ions, such as Cu(II),[53] VO(II),[54] and Al(III).[55] In this regard, the possibility cannot be discounted that species such as $[FeLH_{-1}]^+$, $[FeL_2H_{-1}]^0$, and so forth between Fe(III) and quinic acid could form structural binding isomers, in which the coordination sphere of the metal ion is filled by monodentate or bidentate bound quinate, hydroxide, and water ligands. In structures such as $[FeLH_{-1}]^+$ or $[FeL_2H_{-1}]^0$, the additional H_{-1} could emerge upon dissociation of a coordinated water molecule in the coordination sphere of octahedral Fe(III) or even dissociation of the α-OH alcoholate group and coordination of the incipient α-O^- group.

On the basis of the aforementioned grounds, a stepwise formation of $[FeL_2H_{-1}]^0$ from the $[FeLH_{-1}]^+$ species could be logically proposed, according to the equilibrium:

$$[FeLH_{-1}]^+ + L^- \rightleftharpoons [FeL_2H_{-1}]^0 \qquad \log K = 2.67 \quad (3)$$

This value is similar to log K($FeLH_{-1}$) value (2.80), suggesting that likely only one ligand molecule is coordinated by a deprotonated alcoholate. The second ligand molecule is bound to Fe(III) in a (COO^-, OH) fashion. A similar value (log K 3.15) for the above equilibrium could be calculated for the Fe(III)-citrate system.[50] This suggests that coordination of the second quinate ligand to Fe(III) is favored, likely aided by electrostatic attractions between the reacting species $[FeLH_{-1}]^+$ and L^-.

Above pH 3.5, the dinuclear complexes $[Fe_2L_3H_{-4}]^-$ and $[Fe_2L_3H_{-5}]^{2-}$ predominate in the solution equilibria. The major complex in the pH range 3.5−5.8 is the $[Fe_2L_3H_{-4}]^-$ species. The deprotonation of this complex according to the equation

$$[Fe_2L_3H_{-4}]^- \rightleftharpoons [Fe_2L_3H_{-5}]^{2-} + H^+ \qquad (4)$$

bears a pK 8.05 and results in the emergence of a new dinuclear species. Because Fe(III) has been known to deprotonate α-hydroxycarboxylic acids, the deprotonation could refer both to quinate ligands and to the coordinated water molecules. The characteristics of this deprotonation (pK 8.05) reflect a similarity to the deprotonation of the dinuclear species of Fe(III) with 1-phenyl-1-hydroxymethylene bisphosphonate and its analogues (pK 8.6−9.5) at pH values beyond 6.[8]

At pH 4.6, a maximum 85% of the iron is sequestered into $[Fe_2L_3H_{-4}]^-$. In this dinuclear species, the quinate ligands act as bidentate moieties. Three "H_{-1}" moieties could be attributed to the deprotonation of water molecules in the coordination sphere of the two octahedral Fe(III) centers in a dinuclear core species. The fourth "H_{-1}" could be attributed to the deprotonation of the alcoholic moiety of the quinate ligand, basically turning it into a bridge between the two Fe(III) centers.

In the case of a molar ratio of quinic acid: Fe(III) ≤ 3, a precipitate appears at pH over 4.3−4.4, but in the systems with a ratio greater than 3, beyond pH 4.5, a rapid increase of pH is observed until pH ∼ 10.5. In this pH range, where the equilibrium state is reached over a long period of time

(48) Hynes, M. J.; O'Coinceanainn, M. *J. Inorg. Biochem.* **2004**, *98*, 1457–1464.
(49) Améziane, J.; Aplincourt, M.; Dupont, L.; Heirman, F.; Pierrard, J. C. *Bull. Soc. Chim. Fr.* **1996**, *133*, 243–249.
(50) Koenigsberger, L.-C.; Koenigsberger, E.; May, P. M.; Hefter, G. T. *J. Inorg. Biochem.* **2000**, *78*, 175–184.
(51) Byrne, R. H.; Yao, W.; Luo, Y.-R.; Wang, B. *Marine Chem.* **2005**, *97*, 34–48.
(52) Mentasti, E. *Inorg. Chem.* **1979**, *18*, 1512–1515.
(53) Kiss, E.; Kiss, T.; Jezowska-Bojczuk, M. *J. Coord. Chem.* **1996**, *40*, 157–166.
(54) (a) Kiss, T.; Buglyo, P.; Sanna, D.; Micera, G.; Decock, P.; Dewaele, D. *Inorg. Chim. Acta* **1995**, *239*, 145–153. (b) Kilyén, M.; Labádi, I.; Tombácz, E.; Kiss, T. *Bioinorg. Chem. Applic.* **2003**, *1*, 321–332.

(more that 2 min for every point from Figure 8), $[Fe_2L_3H_{-5}]^{2-}$ emerges as a dominant species, with a maximum percentile content of 88% at pH 7.0.

In the last part of the studied domain of pH, from 7 to 10.8, the three species present are $[FeLH_{-3}]^{-}$, $[FeLH_{-4}]^{-2}$, and $[FeH_{-4}]^{-}$, all mononuclear in nature. In the first two cases, the mixed hydroxo species $[FeLH_{-3}]^{-}$ (it begins to appear at pH $\sim$ 5.5), and $[FeLH_{-4}]^{-2}$ (gradually growing from pH 9.5) might exhibit quinate binding isomer modes. The overall stability constant of the $[FeLH_{-3}]^{-}$ species (log $\beta_{11-3} = -7.83$) is higher than that of the corresponding trihydroxo species $[FeH_{-3}]^{0}$ (log $\beta_{1-3} = -12.94$).[17] For this reason, the formation of the iron trihydroxo species ($[FeH_{-3}]^{0}$) is less favored in the same domain of pH as the $[FeLH_{-3}]^{-}$ species. The stability constant of the species $[FeLH_{-4}]^{2-}$ (log $\beta_{11-4} = -19.45$) is higher than that of the tetrahydroxo species $[FeH_{-4}]^{-}$ (log $\beta_{1-3} = -22.49$) but not to the same extent as for the previous two species. Thus, the tetrahydroxo species, as a minor tetrahedral Fe(III) species, is forming at pH > 9 to the extent of less than 2%. For this reason, this species was not drawn into Figure 9.

For these last two mixed hydroxo iron-quinate complexes, up to four water molecules could enter the coordination sphere around each iron ion. Consistent with the possibility of the α-alcoholate group of the quinate being deprotonated in the presence of Fe(III), in $[FeLH_{-3}]^{-}$ species, one potential binding isomer formulation could encompass the central Fe(III) ion with a singly deprotonated quinate and three hydroxides originating from the deprotonation of an equivalent number of bound water molecules. In this case, the coordinated quinate prevents the precipitation of $Fe(OH)_3$. In a second binding formulation, quinate coordinates in a bidentate (COO^{-}, O^{-}) fashion and only two OH^{-} ions are ionized in the coordination sphere of the metal ion. The $[FeLH_{-3}]^{-}$ species is the predominant species of the high pH range. At pH 10.3, around of 85% of iron is bound in this complex. Beyond pH 10, it is possible that a second deprotonation of quinic acid occurs at the α-alcoholate group.[56] In the analogous case of $[FeLH_{-4}]^{2-}$ species, quinate coordinates in a bidentate (COO^{-}, O^{-}) fashion and only three OH^{-} ions are ionized in the coordination sphere of the metal ion. In view of the above remarks, the most likely stepwise deprotonation process

$$[FeLH_{-3}]^{-} \rightleftharpoons [FeLH_{-4}]^{2-} + H^{+} \quad (5)$$

involving both of the above-mentioned species is favored with a log K 2.13.

Bearing in mind the aforementioned data, pFe values (pFe = $-\log[Fe(III)]_{free}$), given in Table 4, could be a more reliable choice for the evaluation of ligand effectiveness[47] when comparisons are made with other Fe(III) binding ligands. That consideration is especially useful when taking into account the protonation constants of the ligand of interest at physiological pH (pH 7.40), with the total ligand concentration being 2−50 times that of the total iron concentration. For the Fe(III)-quinic acid system, pFe values were calculated through the HySS computer program.[57] What could be observed from this table is that for the Fe(III)-quinic acid system, the pFe value is smaller than those for the other listed ligands.[47,8] On the other hand, the pK_a value for quinic acid (3.34) is much smaller than that of the listed ligands. Therefore, it appears that quinic acid acts as a fairly efficient Fe(III) binding ligand.

Table 4. Equilibrium Free Iron Ion Concentrations Expressed As pFe = $-\log[Fe(III)]_{free}$ Calculated at pH 7.4, for 1 μM of Iron and 10 μM of Ligand, Compared with Other pFe Values for Different Ligands

ligand	pFe	reference
Quinic acid	15.8	this work
N,*N*′-bis(3,4,5-trimethoxy-benzyl)-ethylenediamine-N,N‘-diacetic acid	17.2	47
N,*N*′-dibenzyl-ethylenediamine-*N*,*N*′-diacetic acid	18.1	47
ethylenediamine-*N*,*N*′-diacetic acid	18.2	47
1-phenyl-1-hydroxy-methylene-1, 1-bisphosphonic acid	19.8	8
[1-(diethoxyphosphine)-1-hydroxybenzyl]-1-phosphonic acid	17.9	8
1-benzyl-1-hydroxy-methylene-1, 1-bisphosphonic acid	18.9	8
1-hydroxyethane-1,1-bisphosphonic acid	20.5	8

Discussion

Aqueous Binary Fe(III)-Quinate Chemistry. Comprehending the presence and importance of Fe(III) in biological systems and thus in plants, entails in-depth understanding of its relevant aqueous chemistry with interacting ligands-substrates of both low and high molecular mass. In the case of the binary system of Fe(III) with the physiologically relevant low molecular mass ligand quinate, the aqueous chemistry unravels distinct Fe(III)-quinate interactions, projecting chemical and structural identity in the arising species. To this end, the aqueous speciation studies propose a number of discrete and well-formulated Fe(III)-quinate species. The aqueous studies suggest that (a) there appear to exist both mononuclear, as well as dinuclear, Fe(III)-quinate species present throughout the investigated pH range, (b) mononuclear species are the primary components of the speciation distribution at low pH values, whereas both mononuclear and dinuclear species reach their maximum concentration at physiological pH values and beyond, (c) in the entire pH range, the quinate ligand bound to mononuclear species may be singly deprotonated, with the alcoholic group retaining its proton. That is seemingly consistent with the pH-independent behavior of the alcoholic group throughout the pH-range and the retention of that moiety in the crystal structure of the isolated species **1**−**3**. It appears, however, that the quinate ligand bound to the Fe(III) ion could be doubly deprotonated, with the additional proton departing from the α-alcoholic group, thereby giving rise to various binding isomers in solution or serving as a bridge between two Fe(III) ions, promoting dinuclear complex formation. Hence, the nature of the proposed species, mononuclear and

(55) Lakatos, A.; Bányai, I.; Bertani, R.; Decock, P.; Kiss, T. *Eur. J. Inorg. Chem.* **2001**, 461–469.
(56) Allegretti, Y.; Ferrer, E. G.; Gonzalez Baro, A. C.; Williams, P. A. M. *Polyhedron* **2000**, *19*, 2613–2619.
(57) Alderighi, L.; Gans, P.; Ienco, A.; Peters, D.; Sabatini, A.; Vacca, A. *Coord. Chem. Rev.* **1999**, *184*, 311–318.

dinuclear, reflects the diversity of coordination modes of the quinate ligand around a soluble Fe(III) ion. On the basis of these grounds, a well-formulated set of directives is established challenging the synthetic aspects of the chemistry linked to the aqueous binary Fe(III)-quinate system speciation. In this regard, a mononuclear species such as $[FeL_3]^0$ relates to its solution congener species $[FeL_2H_{-1}]^0$, thus projecting suitable targets for a synthetic investigation.

Key to exploration of the chemical reactivity of the present binary system was (a) the use of the Fe(III):quinic acid molar ratio of 1:3, (b) the choice of three different counterions, and (c) the specific optimal pH values of the reactions run (pH 3−3.5). The synthesis of **1**−**3** in aqueous solutions, their isolation, spectroscopic and structural characterization provides a clear case of mononuclear Fe(III) species bearing the physiological substrate quinate. It appears that interaction of quinate with Fe(III), in the presence of three different counterions, leads to octahedral species in all three complexes **1**−**3** in the solid state. In all cases, the ionization state of the quinate ligand is in correspondence with the oxidation state of the metal ion. The singly ionized form of quinic acid $(C_7H_{11}O_6)^{1-}$ derives from the deprotonation of the α-carboxylate group, with the alcoholic group remaining protonated. As a result of this interaction, a five-membered cyclic ring is formed, rendering the arising species quite stable. Hydroxide ions and/or water molecules of crystallization in **1**−**3** participate in the establishment of extensive hydrogen-bonding interactions throughout the corresponding lattices, contributing to the overall stability of the respective compounds. The physicochemical characterization of **1**−**3** reflected quite elegantly the inherent properties of the $[Fe(C_7H_{11}O_6)_3]^0$ species under investigation in the solid state. The Mössbauer offered an affirmation of the oxidation state of the iron in the mononuclear assembly. The magnetic susceptibility studies defined well the magnetic properties of the species in the solid state, corroborating the EPR measurements in the solid state. The latter spectroscopic technique in the solid state and in solution lent credence to the X-ray crystallographic studies and the aqueous solution speciation studies, projecting the variable yet distinct structure of the Fe(III)-quinate species in the two (solid and solution) states.

The information provided by the multifaceted characterization of **1**−**3** reflects an important feature of the Fe(III) assembly in solution: that there is a neutral charge on the likely complex form $[FeL_2H_{-1}]^0$ arising upon dissolution of **1**. It suggests that the produced aqueous species can traverse cellular structures and interact further with both low molecular and high molecular mass targets. Thus, albeit a low pH structural variant, complex **1** (or **2** and **3**) provides an expediently soluble form of iron, $[FeL_2H_{-1}]^0$, one that potentially elicits interactions in biologically relevant fluids, not unlike those encountered in plant fluids.

Potential Relevance to Fe(III)-Hydroxycarboxylate Chemistry in Plants. Under growth conditions, when iron involvement is necessary to maintain plant physiological processes, iron in soluble and bioavailable forms is essential.[58] Both solubility and bioavailability are attributes intimately associated with the pH-dependent distribution of binary species between Fe(III) and plant fluid physiological substrates exemplified by α-hydroxycarboxylate ligands, such as citrate (xylem sap),[59] malate, lactate, and quinate. To this end, the herein reported aqueous speciation study on the binary Fe(III):quinate system has unravelled discrete species, reflecting the chemistry of solubilization of Fe(III) in the presence of the physiological metal ion chelator quinic acid. Albeit isolated in the low to intermediate pH range, complexes **1**−**3** project structural features consistent with those proposed by the solution speciation study. In this regard, well-defined soluble forms of Fe(III), present in the physiological pH range, could (a) elicit further ternary interactions with low or high molecular mass molecular targets and (b) participate in cellular pathways linked to the homeostatic physiology of lower and higher organisms, including plants.

The ability of quinate to solubilize iron in complex forms similar to or emerging from those of **1**−**3**, enhances its role as an organic cofactor that could contribute to the process of mobilization of iron from plastids to the plant xylem or iron transloading to phloem in plants.[60] To that end, this chemistry relates to the ability of the plant (through its differentiated cell structures) to employ organic substrate-metal ion Fe(III) chemical interactions essential to vital functions.[61,62] Consistent with this line of logic, organic substrates, such as quinic acid, could even reduce free iron toxicity and chemical fixation or the presence of iron as ferric hydroxide and/or oxide.[62]

It is also known that the needs of a plant and its nutritional requirements for essential metal ions are often dictated by environmental adversities[63,64] (e.g., nutritional deficiencies, extreme changes in soil pH, accumulation of other metal ions and substrates, etc.).[65] Under such conditions, chemical responses by plants define key factors[66] affecting solubility and bioavailability of (metallo)nutrients for subsequent uptake and use.[58,64] Therefore, it remains to be seen whether or not binary species characteristics reflected in **1**−**3** could help delineate the molecular chemistry of interactions in Fe(III)-participating events, influencing plant cell physiology.

Conclusions

The pH-specific synthetic chemistry developed herein exemplifies the conditions under which natural metal ion binders can lead to well-defined Fe(III) species such as

(58) Kim, S. A.; Guerinot, M. L. *FEBS Lett.* **2007**, *581*, 2273–2280.
(59) (a) Cataldo, D. A.; McFadden, K. M.; Garland, T. R.; Wildumg, R. E. *Plant Physiol.* **1988**, *86*, 734–739. (b) Pich, A.; Scholz, G.; Seifert, K. *J. Plant Physiol.* **1991**, *137*, 323–326.
(60) Briat, J.-F.; Curie, C.; Gaymard, F. *Curr. Opin. Plant Biol.* **2007**, *10*, 276–282.
(61) Zancan, S.; Suglia, I.; Rocca, N. L.; Ghisi, R. *Environ. Experim. Botany* **2008**, *63*, 71–79.
(62) Rose, A. L.; Waite, D. T. *Geochim. Cosmochim. Acta* **2007**, *71*, 5605–5619.
(63) Reichard, P. U.; Kretzschmar, R.; Kraemer, S. M. *Geochim. Cosmochim. Acta* **2007**, *71*, 5635–5650.
(64) Briat, J. F.; Cellier, F.; Gaymard, F. In *Iron Nutrition in Plants and Rhizospheric Microorganisms*; Barton, L., Abadia, J., Eds; Springer: New York, 2006; pp 345−361.

$[Fe(C_7H_{11}O_6)_3]$ (in **1**−**3**), with distinct chemical and structural properties. Given that metal ion bioavailability is closely linked to the physiological function of a plant cell, the present work supports the idea of soluble well-defined chemical species of Fe(III) bound to quinate, potentially acquiring bioavailability and promoting further ternary interactions at the biological level (iron mobilization and interaction with other low, as well as high, molecular mass molecules such as ferritin). This is in keeping with the solution studies carried out on the specific binary system.

The work on the structural speciation of the binary Fe(III)-quinate system presented only a small token of the number of species present in it. It is logical that other mononuclear and dinuclear species, present as participants in the aqueous speciation of the binary Fe(III)-quinate system that currently elude isolation, constitute targets of currently ongoing research. Through such efforts, it is sought to discover well-defined α-hydroxycarboxylate-bound Fe(III) physicochemical attributes contributing to simple or intricate biological roles of Fe(III) in cellular media.

Acknowledgment. This work was supported by a "PENED" grant co-financed by the E.U.-European Social Fund (75%) and the Greek Ministry of Development-GSRT (25%).

Supporting Information Available: CIF files of X-ray crystal structure refinement data, positional and thermal parameters for $K[Fe(C_7H_{11}O_6)_3]\cdot(OH)\cdot 3H_2O$ (**1**), $(NH_4)[Fe(C_7H_{11}O_6)_3]\cdot(OH)$ (**2**), and $Na[Fe(C_7H_{11}O_6)_3]\cdot(OH)\cdot 8H_2O$ (**3**). This material is available free of charge via the Internet at http://pubs.acs.org.

IC800356V

(65) Hiltbrunner, E.; Flückiger, W. *Tree Physiol.* **1996**, *16*, 963–975.
(66) Grotz, N.; Guerinot, M. L. *Biochim. Biophys. Acta* **2006**, *1763*, 595–608.